Termination Factor for Iterative Noise Reduction in MRI Images Using Histograms of Second-order Derivatives

W. T. Chan, and K. S. Sim

***Abstract*— Histograms of second-order derivatives are generated from the pixel data of MRI images. The histograms are then used to calculate a factor that is to be used for iterative processing. The factor is intended to limit the number of iterations, with the goal of preventing further loss of detail. The factor uses two conditions that depend on the profiles of the histograms. The methodology uses sample MRI images and versions of these images with Rician noise introduced into them. The noisy images are subjected to iterative noise reduction with a recursive averaging filter. The control tests in the methodology use the ground truth images to limit the number of iterations, with PSNR and SSIM peaks used as the measurements for determining when the iterations stop. The other tests use the proposed termination factor for the limitation. The results of the tests are compared to determine the effectiveness of the termination factor. The proposed termination factor does not cause divergence, but there are still different numbers of iterations in the case of MRI images with image subjects that have discrete regions and details resembling noise. The tests also reveal that differences between the histograms of derivatives and Laplace curves have to be retained in order to prevent loss of information.**

***Index Terms*—second-order derivatives, histograms, Laplace curves, MRI images, iterative processing, termination factor, termination conditions**

I. Introduction

THE second-order derivatives of pixels in an image provide information on the variation of details between pixels. These observations have been utilized in previous research about contrast measurement [1] and noise reduction [2]. As changes are implemented on the images, the changes in the second-order derivatives of the pixels exhibit noticeable patterns that can be utilized in equations for convolution techniques. Specifically, this pattern occurs in the frequency histograms of the second-order derivatives.

Histograms of derivatives have been used for deterministic techniques, such as a technique to detect image modifications that are intended to work around techniques that use pixel value histograms [3]. This article demonstrates another application of histograms of derivatives, specifically as a termination factor for iterative processing.

Manuscript received September 28, 2020; revised January 15, 2021.
W. T. Chan is with the Faculty of Engineering and Technology (FET), Multimedia University (MMU), Jalan Ayer Keroh Lama, Bukit Beruang, 75450 Melaka, Malaysia. (phone: +606-2523185; fax: +606 - 231 6552; e-mail: wtchan@mmu.edu.my).

K. S. Sim is also with the FET of MMU. (e-mail: kssim@mmu.edu.my).

II. Review of Previous Work & Revision of Theories

Although the aforementioned previous research works have concluded that the histograms of second-order derivatives can be used for image processing techniques [1] [2], the noise reduction method that was described did not perform well at high levels of noise and used more iterations at these levels [1]. The contrast measurement method that was described is conservative and has considerable false negative outcomes [2]. Further revisions to the algorithms for either methods did not result in net improvement.

Therefore, this research intends to revisit certain theories behind the two previous works. Firstly, the theory that is retained is that the shape of the histogram profile has to resemble a Laplace probability distribution function.

Next, the theory to be revised is the theory that a Laplace curve that is generated using the standard deviation of the distribution of second-order derivatives should coincide with the top of the histogram intervals. This was the main theory behind the aforementioned noise reduction method [2] and the basis for the mathematical calculations for the contrast measurement method [1]. Further revision of the methods with retention of this theory did not produce more satisfactory results. Thus, there is the possibility that this theory is not applicable to every image.

The revised theory is presented in this article. The revision is that for any changes within an image to be effective at minimizing loss of detail, there should be retention of certain characteristics of the histogram profile, relative to *two* Laplace curves that are generated using the distribution of second-order derivatives. The characteristics are measured according to three quantities that can be calculated using the differences between the curves and histogram profiles. Incidentally, these quantities are also used as the conditions for a termination factor that is used to test this revised theory. The factor and its conditions will be described in the Methodology section.

III. Methodology

A. MRI Image Samples

The testing of the termination factor uses a set of 150 MRI images from sources such as Radiopaedia, The Cancer Imaging Archives (TCIA) and Science Photo. The images are selected for diversity in the image subjects and circumstances during which the images are generated. Such diversity has been useful for the purpose of model training [4].

B. Second-order Derivatives & Their Histograms

As in previous research concerning histograms of second-order derivatives, the proposed termination factor uses second-order derivatives that are obtained through a two-dimensional Laplacian operator with a 3 × 3 mask on every pixel [1] [2]. In the case of pixels that are on the boundaries of the image, a 3 × 2 mask is used for the vertical edges and a 2 × 3 mask is used for horizontal ones. The pixels on the corners of the image have a 2 × 2 mask used on them instead. In these cases, the equation for the operator is changed to account for the different masks. The values of the derivatives are then used to generate frequency histograms.

Each interval in a histogram corresponds with one of the distinct values of the second-order derivatives. This is for the purpose of relating the interval with a point on the Laplace curve that will be drawn onto the histogram.

Variables that are described in Equations (1) to (4) are calculated from the histograms. These variables are used as conditions for a termination factor. The use of histograms for such a purpose has been established before, e.g. histogram analysis for the control of recursive procedures [5].

C. Laplace Curves on Histogram

As in past works, a Laplace curve is drawn onto the histogram for comparison with the histogram profile [1] [2]. The exception here is that there is a second curve in the revised theory. The dimensions of the two curves are at a ratio of one-to-one with the heights of the histogram intervals. Both curves are generated using the Laplace probability distribution function (PDF), but each uses different data derived from the second-order derivatives of the pixels.

The first curve uses the standard deviation of the distribution of the second-order derivative values. The results from the Laplace PDF are then multiplied by the number of the pixels in the image.

Each point on the curve corresponds with an interval in the histogram. The height of that point is compared with the height of the interval. The height of the interval represents the frequency of the second-order derivative value that corresponds to the interval, whereas the height of the point on the curve represents a theoretical frequency.

The peak of the second curve coincides with the top of the histogram interval for this second-order derivative value. The standard deviation of the second curve is calculated from this frequency value using Equation (1). For most images, the second curve has a standard deviation of distribution that is different from that of the first curve.

There is the MRI image that is shown in Fig. 1(a), credited to Medscape. Its histogram of second-order derivatives and the two aforementioned curves are shown in Fig. 1(b). The first curve has a standard deviation of 51 and closely follows the histogram profile in the case of this image, whereas the second curve has a standard deviation of 4 and is narrower.

D. Calculations using the Laplace Curve

Both Laplace curves are generated using the Laplace PDF. Equation (1) shows the variables that are involved in this generation.

$$h(j|\mu, b) = N\left(\frac{1}{2b} exp\left(-\frac{|j-\mu|}{b}\right)\right) \qquad b = \frac{\sigma}{2^{0.5}} \tag{1}$$

Where j is a distinct second-order derivative value,
h is the height of the curve corresponding to j,
μ is the average of the second-order derivatives,
σ is the standard deviation that is used and,
N is the number of pixels in the image.

In the case of the first curve, σ is the standard deviation of the distribution; this is designated σ_1 for ease of reference. In the case of the second curve, its standard deviation is designated σ_2. It is found by incrementing or decrementing σ_1 in an iterative process and then generating other curves. When one of these curves has a peak that coincide with the top of the histogram interval that correspond to the second-order derivative value of 0, i.e. $h(0)$ is equal to the frequency of that value, the process ends and the final value of σ_2 is determined to be the value that generated the last curve. This step in the methodology should not be confused with the iterative process that is to be controlled with the termination factor, which will be described later.

Changes to the use of the Laplace PDF have been utilized before for computational algorithms [6]. In this case, the second curve has been generated for the purpose of implementing a condition for the termination of iterations.

E. Differences between Heights of First Curve and Heights of Histogram Intervals

The aforementioned past works utilize the histogram of second-order derivatives and the first Laplace curve.

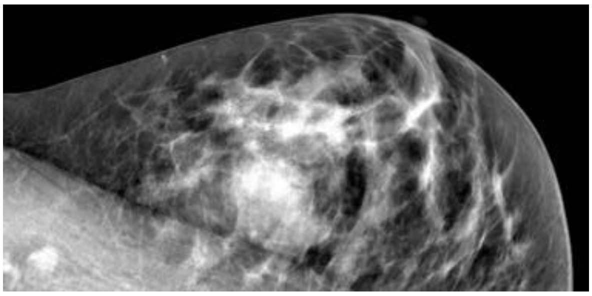

Fig. 1(a): MRI image of breast fibroadenoma

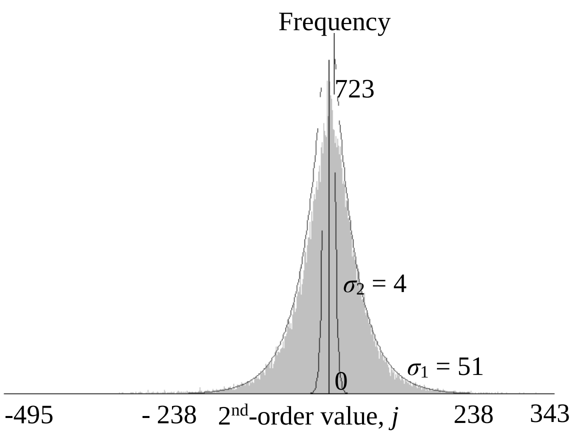

Fig. 1(b): Histogram of second-order derivatives for Fig. 1(a) with both Laplace curves

They asserted that greater differences between the heights of the curve and the heights of the intervals imply poorer image quality, e.g. greater noise or lesser contrast [1] [2]. This article intends to reprise that assertion by having those differences be one of the conditions for termination.

Every location in the first curve corresponds with one of the histogram intervals. The difference between the height of that location and the height of the interval is the variable in this condition. The difference is calculated through Equation (2). This equation has appeared in the work for the aforementioned contrast measurement method, albeit with different notations [2].

$$x_j = h_j - f_j \tag{2}$$

Where j is a distinct second-order derivative value,
f_j is the frequency of j,
h_j is the height of the first curve at the location of j, and
x_j is the aforementioned difference.

F. Condition No. 1: Absolute Value of Sum of Signed Differences

In Equation (2), the difference x_j is signed. The sum of the signed differences across the range of the histogram is obtained. The absolute value of the sum is designated as S. This calculation is shown in Equation (3).

$$S = \left|\sum_{n}^{m} x_j\right| = \left|\sum_{n}^{m} h_j - f_j\right| \tag{3}$$

Where m and n are the boundaries of the range of j.
The other variables have been explained in Equation (2).

A low value of S is obtained when the shape of the first curve closely follows the top of the histogram intervals, or when the positive and negative differences between the curve and histogram closely balance each other. A high value is obtained when many portions of the first curve are far from the histogram profile and their directions do not balance out. In previous works, this case suggests that the image has low contrast or significant noise [2].

The value of S is used as the first condition of the proposed termination factor. If the value of S that is calculated from the results of the current iteration is smaller than the value of S from the previous iteration, the iterations continue. However, during the development of the factor, the condition with S alone did not lead to satisfactory results, e.g. there were more iterations than were needed. Hence, another condition has to be introduced.

G. Condition No. 2: Difference between the Standard Deviations of the Two Laplace Curves

As mentioned earlier, there are two Laplace curves that have been generated using data from the histogram. They have different standard deviations.

During research into the use of histograms of second-order derivatives, there is the observation that images may become blurry after too many iterations of noise reduction, or oversaturated after too much contrast increase.

Incidentally for some of these outcomes, the first Laplace curve approximately reaches the shape of the histogram profile, which was the intended goal of the previous theory [1] [2]. These outcomes contradicted the previous theory.

Therefore, the second condition is that the shape of first Laplace curve must maintain its differences with the silhouette of the histogram profile. Yet, this happens to contradict the aforementioned first condition.

Therefore, there has to be another way to compare the histogram profile with a Laplace curve. This other way involves the approximation of the histogram profile as another Laplace curve. Hence, there is the second curve as shown in Fig. 1(b).

The first condition already uses the differences between the points of the first curve and the heights of the histogram intervals. Thus, the second condition uses the absolute difference between the standard deviations of the first and second curves as the variable for the comparison.

$$\Delta\sigma = |\sigma_1 - \sigma_2| \tag{4}$$

Where σ_1 is the standard deviation of the first curve,
σ_2 is the standard deviation of the second curve, and
$\Delta\sigma$ is the absolute difference between σ_1 and σ_2

The second condition is that $\Delta\sigma$ from the results of the current iteration must be greater than the $\Delta\sigma$ from the results of the previous iteration for the iterations to continue. This condition represents the need to partially retain differences between the first Laplace curve and the histogram profile.

H. Introduction of Noise in MRI Image Samples for Tests

Rician noise is introduced into the aforementioned 150 sample MRI images. The introduction of Rician noise is used in the methodology because noise in MRI images has a Rician distribution [7]. The Rician noise is generated and applied according to gradually increasing standard deviations of distribution, starting from 2. The standard deviations used are 2, 4, 6, 8, 10, 12, 16 and 20. This procedure is intended to test the effectiveness of the termination factor at varying levels of noise. Consequently, each sample MRI image has 8 versions of itself with introduced noise. Therefore, there are 1200 noisy images, plus the aforementioned 150 sample images, which are used as ground truth. An example of a noisy version of the MRI image in Fig. 1(a) is shown in Fig. 2.

I. Iterative Process Used to Test Termination Factor

Recursive processes have been used for reducing the noise in medical images, including MRI images [8]. Therefore, in accordance with this established practice, the iterative

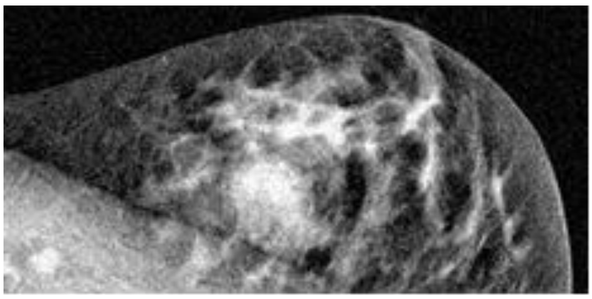

Fig. 2: MRI image in Fig. 1(a) with Rician noise at standard deviation of 20

process that is selected for the testing of the termination factor is the recursive-averaging filter. The filter is applied on the aforementioned noisy images. Each application of the filter on an image is an iteration. The calculations that are involved in the implementation of the termination factor occur before the start of the iterations and after every iteration.

The following is a summary of the conditions for the iterations to continue:

1. Equation (3): S of the current iteration is lower than the S of the previous.
2. Equation (4): $\Delta\sigma$ of the current iteration is greater than the $\Delta\sigma$ of the previous.

If any of the conditions is not met, the iterative process terminates. In the case of the first iteration, S, D and $\Delta\sigma$ from the first iteration are compared with those of the ground truth image.

J. PSNR, SSIM & Control Tests

PSNR and SSIM scores are used to measure the results of every iteration. The PSNR and SSIM are calculated using the aforementioned 150 sample MRI images as ground truth.

The control tests are performed like the iterations that use the proposed termination factor. However, their termination conditions use the PSNR and SSIM scores of the images, before and after each iteration in the control tests. If either the PSNR or SSIM score decreases after an iteration, the iterative process for the control test ends and the results of the previous iteration are used as the outcome. The reason for this is that a decrease in either of the two scores indicates loss of detail [9].

K. Goal of Testing & Hypotheses

Ideally, the proposed termination factor should end the iterative process at the same iteration as the control tests. In such a case, the termination factor is considered to be precise in gauging when to stop the process before any further iterations affect the results and after enough iterations have been performed to achieve optimal outcomes, i.e. the highest PSNR and SSIM scores that can be achieved with the iterative process. Such an outcome would mean that the proposed factor has been efficient at reducing noise.

There is also the possibility of differences in the numbers of iterations between the tests with the factor and the control tests. These differences are used as the measurement of the effectiveness of the factor. Differences between the numbers of iterations determine how far the proposed termination factor is from the ideal outcome. Differences of greater magnitude suggest that the factor has ended the iterative process earlier or later than is optimal.

IV. Results & Discussion

A. Example of Implementation of Termination Factor

The MRI image in Fig. 1 and its noisy versions are used as an example to demonstrate the proposed factors. Table I shows the results for the tests on the image. The results for the control tests are represented by the second column from the left in Table I. Results of the tests with the proposed termination factor are represented by the third column.

Fig. 2 shows the image in Fig. 1 with Rician noise at standard deviation of 20. The results for this noisy image have been highlighted in Table I; they are in the last row. The last row in Table I shows that the iterative process with the control test ended after two iterations. The iterative process with the proposed factor also ended after two iterations. Therefore, in the case of the noisy image in Fig. 2, the outcome is optimal, i.e. the proposed factor terminated the iterative process at the highest PSNR and SSIM that can be achieved with the iterative process. This result also occurs for noise levels of standard deviation 10 and higher, as shown in the fourth to seventh rows of Table I.

However, at lower noise levels, i.e. the first to fourth row of Table I, the tests with the termination factor used either one more or one less iteration than the control tests. Therefore, in the case of the MRI image in Fig. 1, the proposed termination factor does not appear to achieve optimal outcomes for these noise levels.

To investigate the result further, there are the PSNR and SSIM scores for the resulting images. Table II shows the PSNR and SSIM scores for the image in Fig. 1 and its noisy versions. The columns represent the highest PSNR and SSIM scores achieved by the tests.

TABLE I
NUMBER OF ITERATIONS FOR THE TEST ON THE MRI IMAGE IN FIG.1 ACROSS DIFFERENT NOISE LEVELS

Standard deviation of noise distribution in noisy MRI image	Number of iterations to reach highest PSNR or SSIM with control tests	Number of iterations before termination with proposed method
2	0	1
4	1	0
6	1	2
8	3	2
10	2	2
12	2	2
16	2	2
20	2	2

TABLE II
PSNR & SSIM SCORES FOR THE MRI IMAGE IN FIG.1 ACROSS DIFFERENT NOISE LEVELS

Standard deviation of noise distribution in noisy MRI image	Highest PSNR achieved with control tests	Highest SSIM achieved with control tests	PSNR after end of iterations with proposed method	SSIM after end of iterations with proposed method
2	42.35	0.9995	39.89	0.9992
4	37.42	0.9986	36.48	0.9983
6	35.06	0.9976	34.62	0.9974
8	33.05	0.9963	33.03	0.9962
10	31.56	0.9947	31.56	0.9947
12	30.20	0.9927	30.20	0.9927
16	27.77	0.9873	27.77	0.9873
20	25.88	0.9803	25.88	0.9803

The second and third columns have the results from the control tests, whereas the third and fourth have the results from the tests with the proposed factor.

In the case of the image in Fig. 1 and its noisy versions, the iterative process produces gradually decreasing PSNR and SSIM scores for both tests as noise levels increase. This is expected because high levels of noise require more iterations, which lead to diminishing returns [10]. In the case of the tests with the proposed factor, the PSNR and SSIM scores are lower where the number of iterations is not equal to the number of iterations with the control tests.

The tests on the rest of the 150 sample MRI images have their results tabulated in the manner as shown in Tables I and II. The results for all of the sample images are aggregated into the forms as shown in Table III and onwards.

B. Results of Tests on Sample MRI Images

For concise presentation of the results, the outcomes of the tests are categorized according to three types:

Outcome #1: The tests with the proposed factor used the same number of iterations as the control tests.

Outcome #2: The tests with the proposed factor used more iterations than the control tests.

Outcome #3: The tests with the proposed factor used less iterations than the control tests.

The amounts of images that meet the conditions for the outcomes are represented in terms of proportional percentages. For example, if 75 of the 150 images have outcomes of type #2, this is expressed as 50.00%, i.e. half of the 150 sample images have the tests with the proposed factor using more iterations than the control tests.

All tables have their results arranged according to increasing standard deviations of noise distribution in the noisy images. Therefore, the performance of the termination factor can be assessed according to increasing noise.

Tables III, IV and V show the performance of the proposed method across the 150 sample MRI images. Table III focuses on the proportional percentages of images with outcomes #1, #2 or #3. Tables IV and V happen to show breakdowns of the percentages in Table III.

TABLE III
OUTCOMES OF TESTS ACROSS THE 150 SAMPLE MRI IMAGES

Standard deviation of noise distribution	Proportional percentage (%) of sample MRI images with outcomes of different types		
	Type #1	Type #2	Type #3
2	50.00	40.00	10.00
4	38.67	11.33	50.00
6	20.67	10.00	69.33
8	22.00	5.33	72.67
10	27.33	9.33	63.33
12	38.67	3.33	58.00
16	52.67	4.00	43.33
20	68.00	0	32.00

Tables IV and V focus on the differences in numbers of iterations used by the control tests and the tests with the proposed factor.

For further differentiation, Table IV focuses on the variation between the outcomes of type #3, whereas Table V focuses on the variation between the outcomes of type #2. The variation is measured by the difference in the numbers of iterations used by the control tests and the tests with the proposed method.

Table III shows that the outcomes of type #2 reduce in proportion to the other types as the noise level increases. However, the outcomes of type #1 gradually increase. This means that the proposed termination factor is more effective at minimizing the number of iterations at high levels of noise than at low levels. As for outcomes of type #3, they appear to increase as noise levels increase, but their proportion peaks at moderate levels of noise, e.g. noise with standard deviation of 8, before it reduces. This suggests that the proposed factor is best used at moderate to high levels of noise.

TABLE IV
DETAILS OF TESTS WITH OUTCOMES OF TYPE #2

Standard deviation of noise distribution	Proportional percentage (%) of sample MRI images where the tests with the proposed factor used more iterations than the control test by the following amount		
	1 iteration	2 iterations	≥3 iterations
2	14	24	2
4	8	2.67	0.67
6	9.33	0.67	0
8	5.33	0	0
10	9.33	0	0
12	3.33	0	0
16	4.00	0	0
20	0	0	0

*The sum of the percentages for each row equals the percentage of images with outcome of type #2 at the corresponding row in Table III.

TABLE V
DETAILS OF TESTS WITH OUTCOMES OF TYPE #3

Standard deviation of noise distribution	Proportional percentage (%) of sample MRI images where the tests with the proposed factor used less iterations than the control test by the following amount		
	1 iteration	2 iterations	≥3 iterations
2	10	0	0
4	44	6	0
6	44.67	24.00	0.67
8	38.67	32.67	1.33
10	28.67	30.67	4.00
12	25.33	28.67	4.00
16	29.33	12.00	2.00
20	21.33	6.67	4.00

*The sum of the percentages for each row equals the percentage of images with outcome of type #3 at the corresponding row in Table III.

Tables IV shows that outcomes of type #2 rarely have the tests with the proposed factor using more iterations than the control tests. When they do, they usually use one additional iteration. Furthermore, outcomes of type #2 reduce in proportion as noise level increases, which corroborates the finding from Table I. This suggests that the proposed termination factor is conservative in the use of iterations, which is the intended goal of the development of the factor.

Sample MRI images with details that resemble salt and pepper noise comprise most of the outcomes of type #2. An example of such MRI images is shown in Fig. 4. Incidentally, MRI images of fruits and other plant matter happen to have outcomes of this type more often than images with other subjects. This is because details such as the seeds of fruits happen to resemble salt and pepper noise.

The details that resemble salt and pepper noise increase the differences between the histogram profile and the Laplace curves. In turn, this leads to the first condition as described in Equation (3). This suggests that the proposed termination factor should not be used on images with details that resemble salt and pepper noise.

Table V shows that outcomes of type #3 are rare at low levels of noise, but increase in occurrence as noise levels increase. Their frequency peaks at moderate levels of noise, and then reduces afterwards.

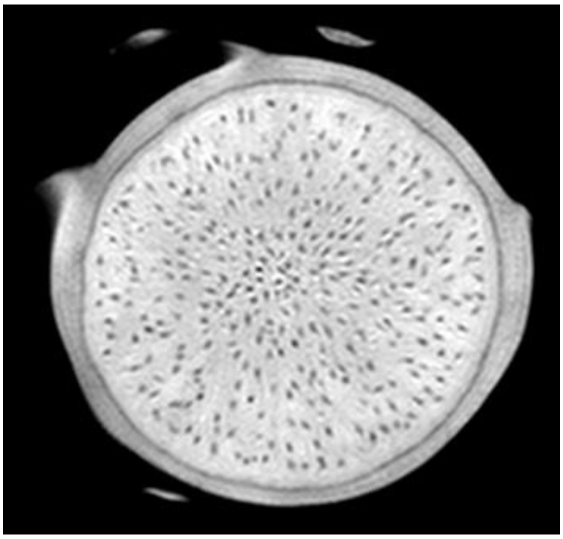

Fig. 4: MRI image of a dragon fruit

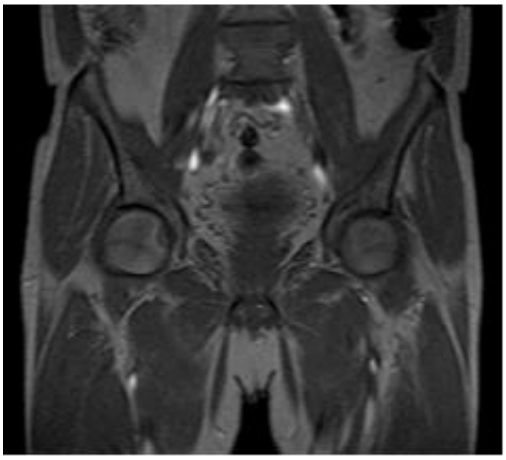

Fig. 3: MRI image of pelvis

Again, this corroborates the findings from Table I. However, this trend only applies for occurrences where the control tests use one or two more iterations than the tests with the proposed factor. For occurrences where the control tests with the factor used more than two iterations, the proportional percentage of these is small but consistent at moderate to high levels of noise. This corroborates the aforementioned suggestion that the proposed termination factor is conservative, albeit not optimally so in these cases.

Sample MRI images with outcomes of type #3 are observed to have many discrete regions. An example is the MRI image of a pelvis (credited to Pueblo Radiology) as shown in Fig. 3. Coronal cross sections are a significant subset of these images. The tests with the termination factor preserve the borders between the regions by stopping the iterations before these borders blur, hence the significant occurrences of outcomes of type #3.

Outcome of types #2 and #3 result in the image having PSNR and SSIM scores that are different from those that are achieved by the control tests. The differences in the scores vary significantly from image to image, but the scores from the tests with the factor are generally lower than the scores from the control tests. Therefore, for more concise presentation of the differences, the scores from the tests with the proposed factor are presented as proportional percentages of the scores from the control tests, as shown in Table VI.

Table VI shows that tests with the proposed termination factor is less effective at achieving the highest possible PSNR scores than it does for SSIM scores. However, the proportional percentages for PSNR scores increase in the case of outcomes of type #2 as noise level increases. The converse occurs for outcomes of type #3.

Recalling Table II, outcomes of type #2 occur less as noise levels increase, whereas outcomes of type #3 occur more often. This suggests that the proposed factor becomes more conservative as noise levels increase, but its performance at improving the quality of the image diminishes.

TABLE VI
DIFFERENCES IN THE PSNR & SSIM SCORES BETWEEN THE CONTROL TESTS AND TESTS WITH THE PROPOSED FACTOR IN TERMS OF PERCENTAGES

Standard deviation of noise distribution	Highest PSNR Scores from Tests with Proposed Factor as Proportional Percentages of Highest PSNR Scores from Control Tests According to Outcome Types (%)		Highest SSIM Scores from Tests with Proposed Factor as Proportional Percentages of Highest SSIM Scores from Control Tests According to Outcome Types (%)	
	Outcome #2	Outcome #3	Outcome #2	Outcome #3
2	89.80	98.47	99.83	99.97
4	95.39	95.93	99.85	99.90
6	97.34	94.15	99.88	99.73
8	98.69	92.95	99.92	99.52
10	98.88	92.40	99.92	99.22
12	98.82	92.07	99.87	98.94
16	99.39	93.79	99.93	98.94
20	-	93.96	-	98.63

As for the SSIM scores, the tests with the proposed factor consistently achieves 99.8% of the highest possible SSIM scores for outcomes of type #2. However, in the case of outcomes of type #3, the percentages have a small but noticeable decreasing trend, though the percentages remain over 98%. This suggests that the proposed factor is effective at optimizing SSIM scores. In turn, this also suggests that the proposed factor is effective at minimizing loss of detail, which is the intended goal.

As for which conditions lead to which outcomes, outcomes of type #1 are caused by either the second condition being broken, or both. There are no cases where the first condition is broken alone. This affirms the need for the second condition to limit the number of iterations. In addition, the occurrence of the second condition being broken alone is notably less frequent than both conditions being broken for outcomes of this type.

As for outcomes of types #2 and #3, there are no discernible patterns between the conditions and the image subjects. There are also no observable trends between the ratios of the conditions types to each other.

V. CONCLUSION & RECOMMENDATION

The proposed termination factor did not cause any divergence, i.e. the iterative process that it is supposed to stop does eventually come to an end. Therefore, the conditions for the factor as described in Equations (1) to (4) are functional at stopping iterative processes like the recursive averaging filter that is used in the tests.

However, the conditions are not as effective on MRI images that contain details that resemble salt and pepper noise, such as cross sections of fruits with seeds as shown in Fig. 4. These images accounted for most of the outcomes of type #2, where the additional iterations due to the factor would cause the iterative process to diminish these details. However, at higher levels of noise, the factor becomes better at preventing these losses.

Furthermore, the termination factor is conservative with regard to images with discrete regions, such as MRI images with coronal dorsal and ventral cross sections. This comprises the majority of outcomes of type #3, where the fewer iterations due to the factor would cause some noise to be retained.

The previous theory about noise and contrast of images was that the Laplace curve that is generated with the standard deviation of the distribution of second-order derivatives should match the shape profile of the histogram of the derivatives. The findings from the tests with the proposed termination factor, specifically the outcomes of type #1, show that this theory is not applicable to every intensity image. Instead, certain differences between the curve and the histogram have to be maintained in order to preserve visual information in the image. Moreover, there have to be two curves, both generated using data from the distribution of second-order derivatives. Thus, the revised theory that introduces these elements has addressed the contradictions of the previous theory.

REFERENCES

[1] W.T. Chan, K.S. Sim & F.S. Abas, "Contrast Measurement with Histograms of Second-order Derivatives of Pixels for Magnetic Resonance Images," Engineering Letters, vol. 27, no. 2, pp. 390-395, 2019.

[2] W.T. Chan, K.S. Sim & F.S. Abas, "Pixel Filtering and Reallocation with Histograms of Second-order Derivatives of Pixel Values for Electron Microscope Images," International Journal of Innovative Computing Information and Control, vol. 14, no. 3, pp. 915-928, 2018.

[3] S. Bharathiraja & B. Rajesh Kanna, "Anti-Forensics Contrast Enhancement Detection (AFCED) Technique in Images Based on Laplace Derivative Histogram," Mobile Networks and Applications, vol. 2019, no. 24, pp. 1174–1180, 2019.

[4] Y. Gao, Y.Y. Wang & J.H. Yu, "Optimized Resolution-Oriented Many-to-One Intensity Standardization Method for Magnetic Resonance Images," Applied Sciences, vol. 9, no. 24, pp. 5531, 2019.

[5] J.W. Han, M. Kamber & J. Pei, "Data Preprocessing," Data Mining (Third Edition), Morgan Kaufmann, pp. 83-124, 2012.

[6] J. Varghese & K.K. Jose, "Wrapped hb-skewed laplace distribution and its application in meteorology," Biometrics & Biostatistics International Journal, vol. 7, no. 6, pp. 525–530, 2018.

[7] C. Pal, P. Das, A. Chakrabarti & R. Ghosh, "Rician noise removal in magnitude MRI images using efficient anisotropic diffusion filtering," BioMedical Engineering OnLine, vol. 27, no. 3, pp. 248 – 264, 2017.

[8] S.U. Saoji & M.V. Sarode, "Speckle and Rician Noise Removal from Medical Images and Ultrasound Images," International Journal of Recent Technology and Engineering (IJRTE), vol. 8, no. 5, pp. 1851 – 1854, 2020.

[9] A. Horé & D. Ziou, "Image Quality Metrics: PSNR vs. SSIM," 20th International Conference on Pattern Recognition, DOI: 10.1109/ICPR.2010.579, 2010.

[10] S.D. Desai & L. Kulkarni, "A Quantitative Comparative Study of Analytical and Iterative Reconstruction Techniques," International Journal Of Image Processing (IJIP), vol. 8, no. 4, pp. 307 – 319, 2010.